Structure−Properties Relation for Agarose Thermoreversible Gels in Binary Solvents

Mohamed Ramzi,[†] Cyrille Rochas,[‡] and Jean-Michel Guenet*,[†]

Laboratoire de Dynamique des Fluides Complexes,[§] Université Louis Pasteur, CNRS UMR 7506, 4, rue Blaise Pascal, 67070 Strasbourg Cedex, France, and Laboratoire de Spectromètrie Physique, Université J. Fourier, CNRS UMR 5588, BP87, 38402 Saint Martin D'heres Cedex, France

Received January 29, 1998; Revised Manuscript Received March 30, 1998

ABSTRACT: The structure of agarose gels prepared in aqueous binary solvents has been studied by means of X-ray and neutron small-angle scattering. The scattering curves are interpreted by considering a random assembly of straight fibers displaying cross-section polydispersity. The cross-section polydispersity is well accounted for with a distribution function of the type $w(r) \sim r^{-\lambda}$ bounded by two radii, r_{min} and r_{max}, and where λ depends upon both the nature of the binary solvent and the agarose concentration. Departure from the Porod regime at wide scattering angles suggests the existence of free and/or dangling chains that do not participate in the network elasticity (*loose* chains). The fraction of loose chains gradually vanishes upon increasing the agarose concentration. Experimental elastic modulus−concentration relations obtained on the same type of samples point to the occurrence of entropic elasticity once analyzed in light of the existence of loose chains. Entropic elasticity is rather consistent with disorganized gel junctions.

Introduction

Agarose gels have been extensively studied these past 30 years, yet they still remain a matter of controversy. Earlier investigations by Rees and co-workers[1,2] had suggested the occurrence of double helices that aggregate to produce a three-dimensional network. This statement was based on an analogy with ι-carraghenans, yet it relied in the case of agarose on X-ray diffraction patterns displaying but a few reflections. Recent studies by Foord and Atkins[3] and Guenet et al.[4] have questioned the very occurrence of this helical structure in agarose gels. Foord and Atkins' improved diffraction patterns obtained with highly stretched agarose gels can only be interpreted by means of single helices. A loose helix of the same type has been contemplated by Guenet et al. to account for the scattering curve obtained from the sol state that further points to a very rigid chain of persistence length larger than 9 nm. The existence of a loose helix in the sol state together with a high persistence length led these authors to wonder how a double helix could eventually be produced during the gelation process, whereas a mere alignment of those single helices would probably be more efficient.

The helical form is not the only item that is now being reconsidered. We have recently suggested[5] on the basis of temperature−composition phase diagrams that ternary complexes are most probably formed (*agarose/water/cosolvent*). Within the gel fibers, agarose chains are therefore organized together with solvent molecules. This type of organization is liable to have a direct bearing upon the gel molecular morphology in the nanometer range. So far, little attention has been paid to this question, apart from some electron microscopy investigations[6−8] and a detailed small-angle X-ray scattering by Djabourov et al.[9] The conclusions drawn by these authors have already been, however, questioned in a recent monograph.[10]

The purpose of this paper is to report on a study of the gel structure which is intended to complement our former thermodynamic study by calorimetry.[5] By using appropriate theories developed for rigid gels,[11] we shall further attempt to establish the relation between the rheological properties and the mesoscopic structure.

Experimental Section

(1) Materials. The agarose sample used in this study was kindly supplied by Hispanagar (Burgos, Spain). Its molecular weight as determined by viscometry measurements[12] was $M_v = 1.12 \times 10^5$, with a water content of about 12.7%.

The sulfate content supplied by the manufacturer was 0.1%. The methyl content as measured by ^{1}H NMR was found to be lower than 0.7%. No L-galactose 6-sulfate was detected by ^{1}H NMR and ^{13}C NMR.

The solvents were purchased from Aldrich and were used without further purification. Bisdistilled water was used. The following abbreviations will be employed throughout the paper: dimethyl sulfoxide = DMSO; *N*,*N*-dimethyl formamide = DMF; *N*-methyl formamide = MF; and formamide = FOR.

(2) Small-Angle X-ray Scattering. SAXS experiments were performed at room temperature on the D24 instrument located at the DCI synchrotron radiation source at LURE (Orsay, France), as well as on the D2AM beam line at the ESRF (Grenoble, France). The experiments were performed at a wavelength $\lambda = 0.149$ nm. A 18-cm linear detector with either 512- or 1024-point resolution together with sample−detector distances of 1.65 and 1.54 m was used at LURE and at ESRF, respectively. Typical acquisition times of 100−400 s were used for a 3% sample at ESRF and LURE, respectively. The spectra of the sample and of the corresponding solvent were recorded in the same cell. After the usual transmission corrections, the solvent spectrum was subtracted from the sample spectrum and the resulting signal was normalized by the detector response, the latter being measured independently.

The sample holder consisted of 30-μm-thick mica windows separated by a 1-mm spacer housed in a stainless steel cell. In order to hinder gelation while the hot solutions (90−100 °C) were being transferred, the cells were kept at 80 °C. The

[†] Université Louis Pasteur.
[‡] Université J. Fourier.
[§] Formerly Laboratoire d'Ultrasons et de Dynamique des Fluides Complexes, CNRS URA 851.

S0024-9297(98)00122-3 CCC: $15.00
Published on Web 08/19/1998

transfer procedure was achieved within a few seconds, and the cells were cooled to room temperature so as to achieve gelation. Under these conditions, solvent evaporation was kept to a minimum.

(3) Small-Angle Neutron Scattering. Small-angle neutron scattering experiments were performed on the PAXE camera located at Orphée (Laboratoire Léon Brillouin, Saclay France). PAXE is equipped with a two-dimensional sensitive detector made up of 128 × 128 cells. This detector can be moved to different positions, which allows variations of the sample−detector distance. A mechanical selector provides a wavelength distribution characterized by a full width at half-maximum $\lambda/\lambda_m \approx 10\%$. By using different sample−detector distances and $\lambda_m = 0.6$ nm, the following q range was made available: $0.1 \leq q\ (\mathrm{nm}^{-1}) \leq 2.5$, with $q = (4\pi/\lambda_m)\sin(\theta/2)$ (θ = scattering angle).

The intensity scattered by agarose in the gel sample, $I_{agarose}$, is written[13] as

$$I_{agarose} = \frac{I_{sample}}{T_{sample}e_{sample}} - (1-\varphi)\frac{I_{solvent}}{T_{solvent}e_{solvent}} - 8.65\varphi\frac{N_p}{V_{agarose}}$$

where I_{sample} is the total scattered intensity, $I_{solvent}$ is the intensity scattered by the binary solvent (both intensities are those obtained after empty cell subtraction and normalization by a totally incoherent scattering sample, i.e., hydrogenous water), T and e, with appropriate subscripts, are the transmissions and thicknesses, and φ is the polymer volume fraction. The third term was determined experimentally by Fazel et al.[13] and stands for the incoherent background scattered by the hydrogenous material on condition that coherent scattering predominates, as is the case here. In this term, N_p is the number of protons in the solution and V_m the molar volume of agarose.

Samples were prepared in hermetically sealed quartz cells of 5-mm optical path, into which the desired quantity of each constituent was introduced beforehand. The mixture was heated at 100 °C while being gently stirred until a clear, homogeneous solution was obtained. The gels were produced by a quench to room temperature.

(4) Mechanical Testing. Measurement of the elastic modulus (E) was achieved on an Instron 4301 through the analysis of the stress−strain curves recorded upon compression. The following relation was used:

$$\sigma = E\epsilon$$

where ϵ is the strain ($\epsilon = l - l_0/l_0$, where l_0 is the sample's initial height) and σ the stress. Experiments were carried out at a rate of 10 mm/mn.

Gels were produced by pouring hot, homogeneous solutions into a cylindrical test tube of 17-mm diameter and about 15-cm length. The gel cylinders were then guillotined out with a razor blade so as to produce samples of 17-mm length and 17-mm diameter suitable for mechanical measurements. A special setup described elsewhere[5] was used for cutting the gels so as to obtain highly parallel faces.

Results and Discussion

(1) Gel Structure. Depending upon the fraction of cosolvent and the agarose concentration, three types of scattering curves are obtained (see Figures 1−3). As can be seen in Figure 1, where the intensity is plotted by means of a $q^4I(q)$ vs q representation, a linear variation is observed up to $q \lesssim 1\ \mathrm{nm}^{-1}$ for agarose/water/cosolvent gels of high water content. Such a behavior can be accounted for through the use of a recent model developed by Guenet for fibrillar gels.[14] In this model, the gel is portrayed as an assembly of straight fibrils displaying cross-section polydispersity. This polydispersity is described by a distribution function of the type $w(r) \propto r^{-\lambda}$ ($0 < \lambda < 3$) bounded by two cutoff radii, r_{min} and r_{max}.

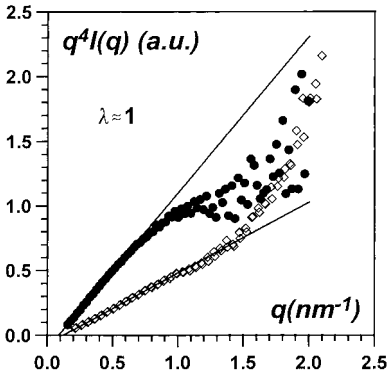

Figure 1. X-ray scattering by gels prepared from water/DMF binary mixtures ($q^4I(q)$ vs q). ● = 70/30 (vol/vol), $C_{agarose} = 5$ g/L; ◇ = 50/50 (vol/vol), $C_{agarose} = 5$ g/L. Case where $\lambda \approx 1$.

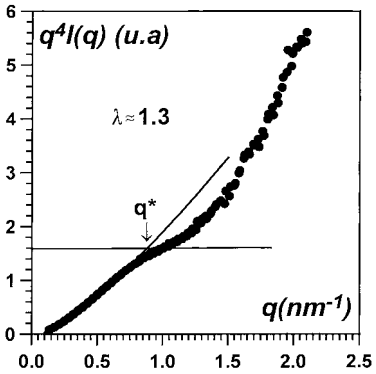

Figure 2. X-ray scattering by a gel prepared from a 30/70 (vol/vol) water/MF binary mixture ($q^4I(q)$ vs q). $C_{agarose} = 20$ g/L. Case where $\lambda \approx 1.3$.

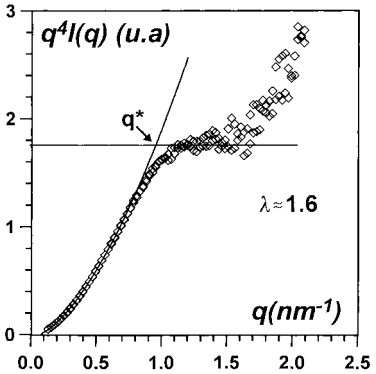

Figure 3. X-ray scattering by a gel prepared from a 30/70 (vol/vol) water/DMF binary mixture ($q^4I(q)$ vs q). $C_{agarose} = 20$ g/L. Case where $\lambda \approx 1.6$.

This model holds provided that $ql_n > 1$ and $l_n > r_{max}$, where l_n is the network mesh size. In order to check whether these two criteria are fulfilled, we have considered the relation mesh size−agarose concentration obtained experimentally by Righetti et al. by determination of the mobility of calibrated latex spheres:[15]

$$l_n = 705C_{agarose}^{-0.7} \quad (1)$$

where l_n is expressed in nm and $C_{agarose}$ in g/L.

Admittedly, no information is, as yet, available as to the mesh size in binary solvents such as those considered in this study. However, as the elastic modulus does

not significantly vary with the cosolvent type and fraction, we may safely assume that the mesh size is nearly given by relation 1 in all cases.

The maximum concentration used in this study was 7% for which relation 1 gives a mesh size $l_n = 36$ nm (for 0.5%, 229 nm; 2%, 87 nm; 3%, 65 nm; 5%, 45 nm). Accordingly, the criterion $ql_n > 1$ is satisfied for all the scattering curves. Further, electron microscopy investigations have never revealed fibers possessing cross sections larger than 10 nm, which entails that $l_n > r_{max}$ is also fulfilled.

Under these conditions, two regimes are expected in Guenet's model: the *transitional regime* and the *Porod regime*. In the transitional regime, the only requirements are those discussed above plus $qr_{max} > 1$. The intensity is then written as

$$\frac{q^4 I_A(q)}{C} 4\pi^2 \rho \left[A(\lambda) q^{\lambda} - \frac{1}{\lambda r_{max}^{\lambda}} \right] / \int_{r_{min}}^{r_{max}} w(r)\, dr \qquad (2)$$

where ρ is the density and $A(\lambda)$ is expressed as follows:

$$A(\lambda) = \frac{\Gamma(\lambda)\Gamma\left(\frac{3-\lambda}{2}\right)}{2\lambda\Gamma\left(\frac{\lambda+1}{2}\right)\Gamma\left(\frac{\lambda+3}{2}\right)\Gamma\left(\frac{\lambda+1}{2}\right)} \qquad (3)$$

A case of particular interest occurs for $\lambda = 1$:

$$\frac{q^4 I_A(q)}{C} = \left[2\pi^2 \rho q - \frac{4\pi\rho}{r_{max}} \right] \frac{1}{\log(r_{max}/r_{min})} \qquad (4)$$

as the variation happens to be linear in a $q^4 I(q)$ vs q representation. This case corresponds to agarose gels in pure water as well as in binary mixtures of high water content for agarose concentrations lower than 2%. Interestingly, the intercept q_0 as obtained by extrapolation of $q^4 I(q)$ to zero is related to r_{max} through

$$\frac{1}{r_{max}} = [\lambda\pi A(\lambda)]^{1/\lambda} q_0 \qquad (5)$$

which, for $\lambda = 1$, reduces to

$$r_{max} = \frac{2}{\pi q_0} \qquad (6)$$

In the Porod regime, the intensity reduces to the well-known form

$$\frac{q^4 I_A(q)}{C} = 4\pi\rho \int_{r_{min}}^{r_{max}} \left[1 + \frac{3}{8q^2 r^2} + \ldots \right] w(r)\, dr / \int_{r_{min}}^{r_{max}} w(r)\, dr \qquad (7)$$

which reaches a constant asymptotic value at large q

$$\frac{q^4 I_A(q)}{C} \cong \frac{4\pi\rho}{r_n} \qquad (8)$$

where r_n is the number-averaged cross-section radius.

The scattering vector, q^*, at which the asymptote of the transitional regime and the Porod regime intersect is written as

$$\frac{1}{r_{min}} = [\lambda\pi A(\lambda)]^{1/\lambda} q^* \qquad (9)$$

Table 1. Values of λ for Different Agarose/Water/Cosolvent at Different Agarose Concentrations (g/L) and Binary Solvent Compositions as Obtained from X-ray Scattering Data (from Neutron Scattering Data for DMSO)

	λ		
water/DMF (v/v)	$C_{agarose} = 0.5\%$	$C_{agarose} = 2\%$	$C_{agarose} = 5\%$
0.7/0.3	1.05 ± 0.05	1.05 ± 0.05	1.2 ± 0.1
0.5/0.5	1.1 ± 0.1	1.3 ± 0.1	1.5 ± 0.1
0.3/0.7	1.6 ± 0.1	1.6 ± 0.1	1.7 ± 0.1
	λ		
water/MF (v/v)	$C_{agarose} = 0.5\%$	$C_{agarose} = 2\%$	$C_{agarose} = 5\%$
0.7/0.3	1.05 ± 0.05	1.05 ± 0.05	1.3 ± 0.1
0.5/0.5	1.1 ± 0.1	1.3 ± 0.1	1.4 ± 0.1
0.3/0.7	1.3 ± 0.1	1.3 ± 0.1	1.4 ± 0.1
	λ		
water/DMSO (v/v)	$C_{agarose} = 3\%$		$C_{agarose} = 7\%$
0.7/0.3	1.05 ± 0.05		1.1 ± 0.1
0.5/0.5	1.3 ± 0.1		1.3 ± 0.1
0.3/0.7	1.6 ± 0.1		1.7 ± 0.1

which, for $\lambda = 1$, reduces to

$$r_{min} = \frac{2}{\pi q^*} \qquad (10)$$

An analysis by means of eqs 2 and 8 has given different sets of values for r_{min}, r_{max}, and λ, the latter values being gathered in Table 1. We note that beyond the Porod regime, another behavior appears whose meaning will be discussed later. The outcomes of the analysis are 3-fold:

(i) As a rule, r_{max} does not vary significantly in all these systems if one takes into account the relative accuracy in determining this parameter by means of relation 5. Typical values are 6−9 nm, with 6 nm being the most frequent value found. Such values are consistent with those obtained from electron microscopy investigations.[6−8]

(ii) The value of r_{min} is less scattered (0.8−0.9 nm). That the Porod regime is reached for $q \approx 0.9$ nm^{-1} is rather consistent with the value of r_{min} as determined by relation 9. This parameter does not vary significantly with solvent type, solvent composition, or agarose concentration. The radius found would correspond approximately to three or four chains in contact if one takes nearly extended helices as those proposed by Foord and Atkins and also considered by Guenet et al.[4,16] for explaining the neutron scattering results of agarose chains in the sol state.

(iii) The values of λ also differ with solvent composition and agarose concentration. Three typical values are observed:

$\lambda \approx 1$ occurs for low contents of cosolvent in the binary solvent and low agarose concentrations (Figure 1).

$\lambda \approx 1.3$ is observed for either high agarose concentrations and low cosolvent content or for high cosolvent content and low agarose concentrations (Figure 2).

$\lambda \approx 1.6$ occurs for a high fraction of DMF or DMSO whatever the agarose concentration is (Figure 3).

Higher values of λ mean that the fraction of fibrils possessing a small cross section is increased. So by increasing either the cosolvent fraction or, in some cases, the agarose concentration, the growth of fibrils with a small cross section is favored. These outcomes may seem to conflict with electron microscopy findings. This technique does not highlight much cross-section poly-

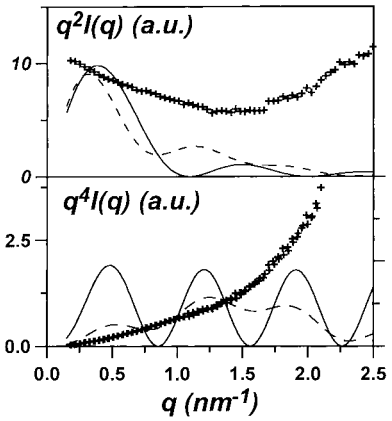

Figure 4. Comparison between the intensity scattered by a gel (presently $C_{agarose} = 5$ g/L in a 50/50 water/DMF mixture) and the theoretical curves calculated by taking a single cross-section radius ($r = 7$ nm) (solid line) and by considering two cross-section radii as proposed by Djabourov et al. (dashed line). In the latter case, $w_1 = 0.42$.

dispersity as fibers of 7 nm in cross section are seen. Yet taking into account only this value does not allow one to reproduce the experimental scattering curve. Indeed, the scattering by very long solid fibers is written[17] as

$$I(q) = \frac{4\pi\mu_L}{q}\frac{J_1^2(qr)}{q^2r^2} \qquad (11)$$

where μ_L is the mass per unit length and r the cross-section radius. The curve obtained for $r = 7$ nm is shown in Figure 4 by means of two different representations. The theoretical curve displays pronounced oscillations which are strongly at variance with the experimental scattering curve for all the systems studied. Clearly, electron microscopy detects only the fibers of cross sections close to r_{max} but misses those of smallest cross section.

Also, the present data are not consistent with a two-population system as proposed by Djabourov et al.[9] The intensity scattered by a binary population of solid fibers is written as

$$I(q) \propto \frac{4\pi\mu_L}{q}\left[w_1\frac{J_1^2(qr_1)}{q^2r_1^2} + (1 - w_1)\frac{r_2^2}{r_1^2}\frac{J_1^2(qr_2)}{q^2r_2^2}\right] \qquad (12)$$

where μ_L is the mass per unit length of rods of radius r_1 and w_1 their weight fraction. Introducing the values proposed by Djabourov et al., i.e., $r_1 = 1.5$ nm, $r_2 = 4.5$ nm, and $w_1 = 0.42$, into eq 12 does not produce a satisfactory fit either (see Figure 4). Evidently, a high degree of cross-section polydispersity, such as considered by Guenet, is required.

Guenet's model does not hold any longer beyond $q = 1.5$ nm^{-1}. Another scattering regime takes over as shown by the departure from $1/q^4$ behavior. This behavior is, however, concentration-dependent, as it gradually vanishes with increasing agarose concentration and is clearly absent when $C_{agarose} = 7\%$ (see Figure 5). This scattering can be attributed to free chains (totally disconnected from the network) and/or to dangling chains (attached by one end to the network). There is no straightforward method to distinguish between either case, so we shall use the term *loose chains* in what follows. In the q range under consideration, these chains are expected to scatter as solid cylinders as decribed by relation 11. As a result, the total scattered intensity should be written[18] as

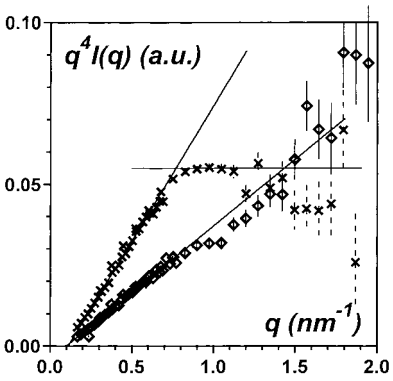

Figure 5. Neutron scattering by gels prepared from D_2O/DMSO-d_8 binary mixtures ($q^4I(q)$ vs q). $C_{agarose} = 30$ g/L (×); $C_{agarose} = 70$ g/L (◇).

$$\frac{q^4I(q)}{C} = X\frac{4\pi\rho}{r_n} + (1 - X)4\pi q\mu_L\frac{J_1^2(qr_H)}{r_H^2} \qquad (13)$$

where X is the volume fraction of the network, $1 - X$ the volume fraction of loose chains, and r_H the chain cross section. This equation has been contemplated on a qualitative basis only, since the unknown value of ρ prevents us from fitting the curve in order to derive X. The value of ρ is dependent upon the stoichiometries of the different complexes, which so far are unknown. Note that traces of loose chains will be easily detected by scattering experiments, as the first term in eq 13 drops very rapidly, unlike the second term. In principle, no plateau regime should ever be observed, as eq 13 is a parabola whose minimum occurs at $q = 0$. The plateau regime can only be observed at very low fractions of loose chains because of the parabola flattening. This, therefore, suggests that beyond 2%, the fraction of loose chains is rather low and finally becomes zero for $C_{agarose} = 7\%$.

Scattering data therefore hint at the existence of a population of chains that is not involved in the elasticity of the network and that gradually disappears while increasing the agarose concentration. This statement has a direct bearing upon the understanding of the rheological properties that are presented next.

(2) Rheological Properties. In this study, only the gel elastic modulus as a function of agarose concentration has been measured for different types of cosolvent at different compositions. The same behavior has been found for all systems and is represented by a typical curve shown in Figure 6. As can be seen, two regimes occur:

regime I $\quad E \sim C^{2.25\pm0.1}$ for $C \lesssim 20$ g/L

regime II $\quad E \sim C^{1.5\pm0.1}$ for $C \gtrsim 20$ g/L

It is worth examining these results in light of Jones and Marquès' theory.[11] This theory relies upon the fractal dimension of the objects connected at the junction of a network. As discussed elsewhere,[16] this approach pertains to agarose gels since $l_n > r_{max}$. The relevant parameter is then *the longitudinal fractal dimension* of the fibers, i.e., the fractal dimension of the contour

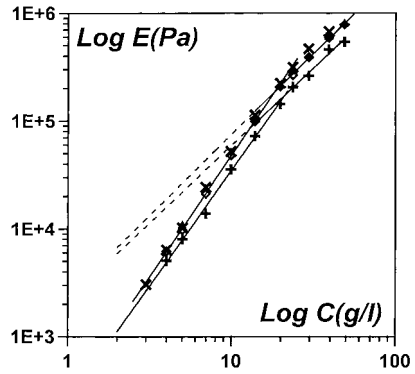

Figure 6. Variation of the elastic modulus (**E**) as a function of the agarose concentration. Here the composition is 50/50 (vol/vol): × = DMF; + = FOR; ◇ = DMSO; ▲ = MF. The same behavior is observed independent of the binary mixture composition.

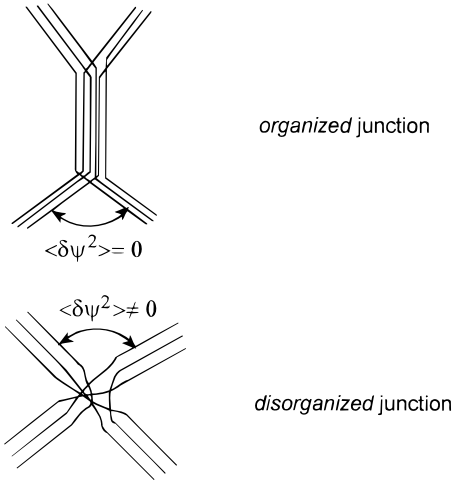

Figure 7. Schematic representation of an organized junction and a disorganized junction.

length related to the fiber long axis. For instance, a straight fiber possesses a longitudinal fractal dimension $D_f = 1$.

This theory distinguishes between two types of elasticity: *entropic* elasticity and *enthalpic* elasticity. Entropic elasticity occurs when flexible objects are involved. These flexible objects can be the chains connected at the junctions or the junctions themselves. In other words, if one considers an angle ψ between two fibers, entropic elasticity occurs if this angle can fluctuate; i.e., $\langle\delta\psi^2\rangle \neq 0$. In the case of fibrillar gels, fibrils are intrinsically rigid so that entropic elasticity can only be observed if the junctions are disordered (see Figure 7). As for enthalpic elasticity, it occurs when the system is totally rigid; i.e., $\langle\delta\psi^2\rangle = 0$.

Jones and Marquès have derived the following relations between the modulus and the network volume fraction:

$$E \propto \varphi^{3/(3-D_f)} \qquad \text{entropic} \qquad (14)$$

$$E \propto \varphi^{(3+D_f)/(3-D_f)} \qquad \text{enthalpic} \qquad (15)$$

where D_f is the longitudinal fractal dimension of the fibers in the present case.

Early experiments[16] for which the second regime at higher concentrations had not been identified led us to conclude that agarose showed essentially enthalpic elasticity with a longitudinal fractal dimension for the fibers of $D_f \approx 1.1$. The appearance of the second regime together with the neutron scattering results presented above lead us to reconsider this interpretation. First of all, it is worth emphasizing that Jones and Marquès' theory relies upon the *network volume fraction*, which can differ from the *polymer volume fraction*. Present scattering results have hinted at the existence of loose chains that do not evidently participate in the elasticity of the network. Clearly, below a given concentration, the network volume fraction is at variance with the polymer volume fraction. Consequently, the relation between the modulus and the polymer concentration does not provide one with an exponent characterizing the network. Conversely, above a given concentration, scattering data suggest that the fraction of loose chains is negligible. We therefore conclude that the exponent found in this range of concentration (1.5 ± 0.1) most probably correctly describes the intrinsic structure of the agarose network.

Under these conditions, only entropic elasticity is liable to yield such an exponent. This leads us to conclude that (i) the junctions are flexible and, hence disordered and (ii) the fractal dimension of the fibers is $D_f \approx 1$, a value borne out by electron microscopy investigations.

Assuming that the departure at low agarose concentrations from the behavior observed at high agarose concentrations arises from those loose chains, then their fraction (X_f) is given by

$$X_f = 1 - 0.235 C_{\text{agarose}}^{\,0.5\pm0.03} \qquad (16)$$

where C_{agarose} is expressed in g/L.

The origin of these loose chains, whose fraction is concentration-dependent, is puzzling. At high concentrations (i.e., $C_{\text{agarose}} > 2\%$), agarose gels can be described with the usual "equilibrium" thermodynamics[5] for multiphasic systems ("equilibium" means that the occurrence of thermal events is not heating or cooling rate-dependent, although their associated temperature is). Normally, as long as no transformation takes place, the different phases should keep the same composition at a given temperature independent of the agarose concentration. Evidently, this is no longer so in the vicinity of the critical gelation concentration, as the composition of the dilute phase varies when altering the agarose concentration.

Gels prepared close to the critical gelation concentration are known to be highly inhomogeneous, a morphology that may be due to hydrodynamic instabilities. Are these instabilities, should they occur and still exist once the gel is formed, capable of peeling off the outer chains of the fibers, resulting in the existence of loose chains? Clearly, unexplained phenomena are most probably taking place near the gelation threshold that still need to be identified and elucidated.

Acknowledgment. We are greatly indebted to E. Geissler and C. Bourgaux for their experimental assistance.

References and Notes

(1) Anderson, N. S.; Campbell, J. W.; Harding, M. M.; Rees, D. A.; Samuel, J. W. B. *J. Mol. Biol.* **1969**, *45*, 85.
(2) Arnott, S.; Fulmer, A.; Scott, W. E.; Dea, I. C. M.; Moorhouse, R.; Rees, D. A. **1974** *J. Mol. Biol. 90*, 269.
(3) Foord, S. A.; Atkins, E. D. T. **1989** *Biopolymers 28*, 1345.

(4) Guenet, J. M.; Brûlet, A.; Rochas, C. **1993** *Int. J. Bio. Macromol. 15*, 131.
(5) Ramzi, M.; Rochas, C.; Guenet, J. M. **1996** *Macromolecules 29*, 4668.
(6) Griess, G. A.; Guiseley, K. B.; Serwer, P. *Biophys. J.* **1993**, *65*, 138.
(7) Griess, G. A.; Edwards, D. M.; Dumais, M.; Harris, R. A.; Renn, D. W.; Serwer, P. *J. Struct. Biol. J.* **1993**, *111*, 39.
(8) Sugiyama, J.; Rochas, C.; Turquois, T.; Taravel, F.; Chanzy, H. *Carbohydr. Polym.* **1994**, *23*, 261.
(9) Djabourov, M.; Clark, A. H.; Rowlands, D. W.; Ross-Murphy, S. B. **1989** *Macromolecules 22*, 180.
(10) Guenet, J. M. *Thermoreversible Gelation of Polymers and Biopolymers*; Academic: London, 1992.
(11) Jones, J. L.; Marquès, C. M. **1990** *J. Phys. (les Ulis) 51*, 1113.
(12) Rochas, C.; Lahaye M.; **1989** *Carbohydr. Polym. 10*, 289.
(13) Fazel, N.; Brûlet, A.; Guenet, J. M. **1994** *Macromolecules 27*, 3836.
(14) Guenet, J. M. **1994** *J. Phys. II 4*, 1077.
(15) Righetti, P. G.; Brost, B. C. W.; Snyder, R. S. *J. Biochem. Biophys. Methods* **1981**, *4*, 347.
(16) Rochas, C.; Brûlet, A.; Guenet, J. M. **1994** *Macromolecules 27*, 3830.
(17) Pringle, O. A.; Schmidt, P. W. **1971** *J. Appl. Crystallogr. 4*, 290.
(18) Guenet, J. M.; Jeon, H. S.; Khatry, C.; Jha, S. K.; Balsara, N. P.; Green, M. M.; Brûlet, A.; Thierry, A. *Macromolecules* **1997**, *30*, 4590.

MA9801220